Title	A dynamic model of the MYCN regulated DNA damage response in Neuroblastoma
Authors(s)	Kuehn, Axel, Kholodenko, Boris N., Fey, Dirk
Publication date	2014-11-05
Publication information	Kuehn, Axel, Boris N. Kholodenko, and Dirk Fey. "A Dynamic Model of the MYCN Regulated DNA Damage Response in Neuroblastoma." IEEE, 2014.
Conference details	IEEE International Conference on Bioinformatics and Biomedicine (BIBM 2014): Workshop on Empowering Systems Medicine Through Optimal Design of Experimentation and Computational Modeling, Belfast, Northern Ireland, 2-5 November 2014
Publisher	IEEE
Item record/more information	http://hdl.handle.net/10197/7783
Publisher's statement	© © 2014 IEEE. Personal use of this material is permitted. Permission from IEEE must be obtained for all other uses, in any current or future media, including reprinting/republishing this material for advertising or promotional purposes, creating new collective works, for resale or redistribution to servers or lists, or reuse of any copyrighted component of this work in other works.

A dynamic model of the MYCN regulated DNA damage response in Neuroblastoma

Axel Kuehn
Systems Biology Ireland
UCD Conway Institute
Dublin, 4
Email: axel.kuehn@ucdconnect.ie

Boris Kholodenko
Systems Biology Ireland
UCD Conway Institute
Dublin, 4
Email: boris.kholodenko@ucd.ie

Dirk Fey
Systems Biology Ireland
UCD Conway Institute
Dublin, 4
Email: dirk.fey@ucd.ie
Telephone: +353 1 716 6310

Abstract—Neuroblastoma is the most common cancer in infancy with an extremely heterogeneous phenotype that is mainly driven by the MYCN oncogene. The *MYCN* transcription factor and its amplification is commonly associated with poor prognosis in patients, although it has also been shown that elevated *MYCN* levels correlates with apoptosis sensitization in cells. HMGA1 is one of MYCN target genes and is involved in triggering apoptosis through a DNA Damage Response (DDR) by inducing ataxia-telangiectasia-mutated (ATM) gene expression. But HMGA1 is also involved in preventing apoptosis by directly binding HIPK2 and decreasing its presence in the nucleus, therefore decreasing phosphorylation of p53 at serine 46 which is required for the activation of p53 apoptotic targets. In this article, we propose a model in which MYCN protein regulates the HMGA1-ATM-p53 and HMGA1-HIPK2-p53 subsystems. Because the molecular details concerning the HIPK2-HMGA1 interaction are uncertain several possibilities were explored in simulations. Our model points towards an important role of MYCN-dependent regulation of HMGA1 expression levels and the subsequent HIPK2 nuclear/cytoplasmic re-localization and led to experimentally testable predictions that can discern between alternative model structures.

I. INTRODUCTION

Neuroblastoma is the most common extracranial solid tumour in childhood and the most common cancer in infancy. It is an extremely heterogeneous disease stratified in low-, intermediate- and high-risk tumours. Whereas low-risk tumours often undergo spontaneous regression, high-risk tumours can be very aggressive despite multi-modal treatments. The *MYCN* gene encodes for MYCN transcription factor and its amplification is commonly associated with high-risk tumours although it has been shown that *MYCN* gene amplification also correlates with apoptosis sensitization. Thus, MYCN seems to have an interesting biphasic effect on Neuroblastoma. In patients, moderately increased MYCN levels are associated with improved prognosis, whereas *MYCN* gene amplification and greatly increased levels are associated with poor prognosis [1], [2]. These MYCN-amplified, highly aggressive tumours usually evade even extensive multimodal chemotherapy resulting in high death rates. Because tumour aggressiveness and evasion to chemotherapy is intimately linked to the cellular DNA damage response (DDR) and p53 [3], we sought to investigate how MYCN affects the p53 DDR in Neuroblastoma.

The protein p53 is a tumour suppressor that regulates the cell fate in response to DNA damage and other stresses [4]. Depending on its response dynamics, p53 can promote DNA repair, senescence or apoptosis. p53 is often mutated or otherwise inactivated in cancer. In Neuroblastoma, p53 mutations are rare (occurring in 5% of cases), indicating that the p53 system is functionally inactivated at the level of upstream or downstream regulators. MYCN is one of these upstream regulators. A particularly attractive hypothesis arising from the clinical data is that MYCN would exert a dual dosage-dependent effect on the p53 system. In this hypothesis, slightly increased MYCN levels would result in an increased p53 DNA damage response whereas excessively increased MYCN levels, such as found in MYCN-amplified tumours, would impair the p53 apoptotic response. Here, we explored whether this hypothesis is theoretically possible.

The p53 system is complex, containing multiple negative and positive feedback loops, which in turn generate complex dynamics ranging from sustained to pulsatile oscillatory responses [4]–[6]. This complexity hinders a straight forward intuitive understanding of the p53 network. Therefore we took a computational systems biology approach and build a dynamic model of the p53 DNA damage response and its regulation by MYCN. In the following, we first describe the implementation of the model and then proceed by exploring its dynamics.

II. MODELS AND METHODS

The response of p53 to DNA damage can be understood as an input-output signal transduction system (Fig. 1), [6]. The input layer consists of ATM which senses the DNA damage. The output or effector layer consists of p53 which depending on its phosphorylation status promotes cell-cycle arrest or apoptosis. When phosphorylated at S46, p53 promotes apoptosis, and this proapototic form of p53 (hereafter referred to as p53-killer) was chosen as output [7]. The core of our model is based on established models in the literature [4]–[6] and is explained briefly in the following.

Upon DNA damage, ATM is phosphorylated at S1981, most likely through DNA-damage induced autophosphorylation [8], [9]. For simplicity, the ATM phosphorylation reaction in our model is dependent on the DNA damage input, but does not describe the detailed autophosphorylation events. S1981 ATM is also involved in inactivating phosphorylation of MDM2 [10], [11] and SIAH1/SIAH2/WSB1 [12], [13] which all lead to activation of p53. Finally, ATM s1981 directly phosphorylates p53 at serine 15 [14], [15]. Due to overlapping
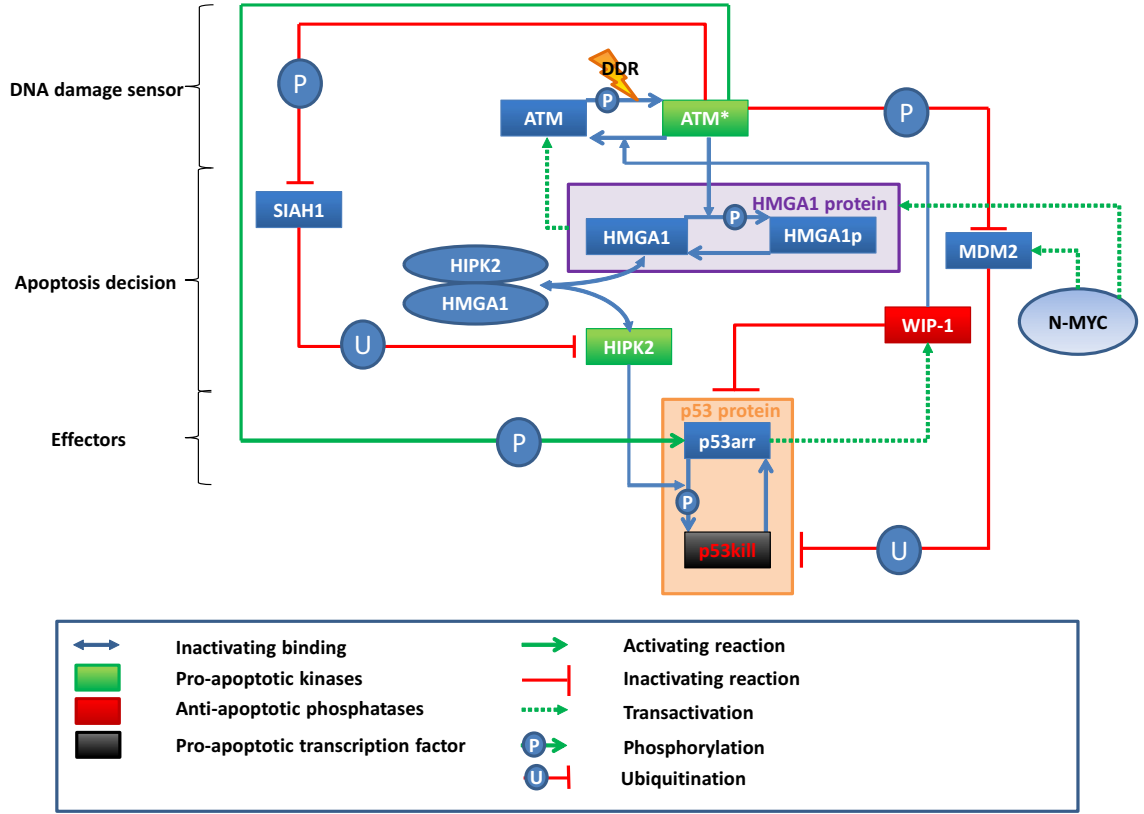
Fig. 1. Schematic of the model.

functions between ATM and ATR, and less efficient kinase activity towards p53, ATR is neglected in this model [14]. By phosphorylating MDM2, ATM S1981 reduces MDM2 binding on p53 which results in decreased MDM2 ubiquitin ligase activity and higher p53 level [11]. Based on [16] we assume that p53 can in turn induce MDM2 gene expression if at least phosphorylated at serine 15, i.e p53 is primarily activated. On the other hand, ATM exerts a similar mechanism on the ubiquitin ligase SIAH1. SIAH1 is responsible for HIPK2 degradation and by phosphorylating SIAH1, ATM reduces the binding affinity between SIAH1 and HIPK2 and allows HIPK2 accumulation [12]. HIPK2 is one of the main kinases involved in p53 serine 46 phosphorylation, also called "p53 killer" [17], [18]. In order for HIPK2 to phosphorylate p53 on serine 46, p53 needs to be first phosphorylated at serine 15 (here referred as the "arrester" conformation) [6], which is achieved by ATM. p53 "arrester" upregulates WIP-1 phosphatase at the transcriptional level. WIP1 dephoshphorylates serine 1981 of ATM [19] and serine 15 of p53 [20]. For a detailed description of this model we refer to the original literature [4]–[6].

In addition to the above described core interactions, our model accounts for the regulation of the p53 system by MYCN. HMGA1 is one of MYCN target genes and is involved in triggering apoptosis through the DDR by inducing ATM gene expression [21]–[24]. But HMGA1 is also involved in preventing apoptosis by directly binding HIPK2 and decreasing its presence in the nucleus, therefore decreasing phosphorylation of p53 at serine 46 which is required for the activation of

p53 apoptotic targets [25], [26]. Taking these experimental observations into account, our extended model includes HMGA1 induced ATM expression [21], ATM/ATR induced HMGA1 phosphorylation [22], HMGA1 dependent HIPK2 cytoplasmic relocalisation [25], [26] and MYCN induced HMGA1 and MDM2 expression [23], [24], [27]. For simplicity, we modelled HMGA1-dependent inactivation and cytoplasmic relocalisation of HIPK2 as a simple sequestration reaction, i.e. HMGA1 binds HIPK2 and the resulting complex is inactive. Because the molecular details for the HMGA1-HIPK2 interaction are uncertain, several possibilities were explored in the model as described in the results section.

Based on the described interactions a dynamic model in form of a system of ordinary differential equations can be derived [28]. This system of ordinary differential equations was implemented and simulated in Matlab. The parameter values were chosen based on established models in the literature and within biologically reasonable bounds [5], [6]. A detailed account of all reactions, rate equations and parameters in the model is provided in Tables I - IV.

In all simulations, we excite the system with a step input of DNA damage at $t = 0$, i.e. $U_{DDR} = 0$ for $t < 0$ and $U_{DDR} = 10$ for $t \geq 0$ and solve the system of ordinary differential equations numerically (Matlab, ode15s solver). To explore the dynamics of the system, interesting static parameters, such as the level of MYCN, are then varied between multiple simulation runs and the resulting output ($p53_{killer}$) trajectories are analysed.
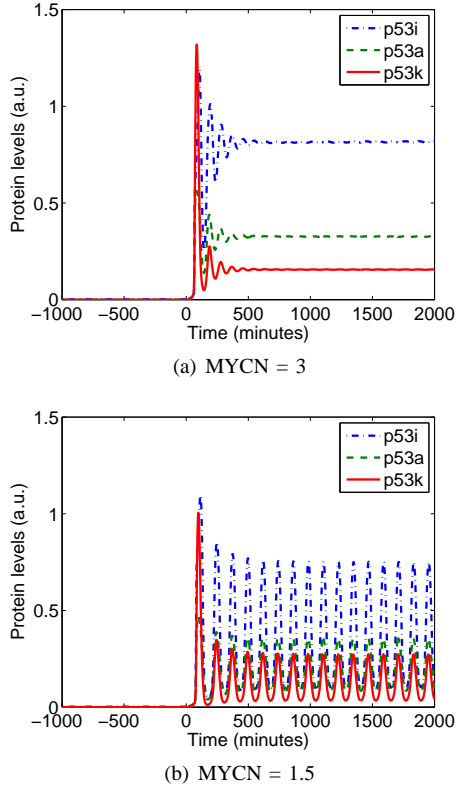
(a) MYCN = 3

(b) MYCN = 1.5

Fig. 2. Time course simulations for different values of MYCN in response to DNA damage $U_{DDR} = 10$ at time $t = 0$. (a) System relaxes to a monostable steady-state. (b) System exhits sustained oscillations. MYCN-dependent MDM2 mRNA synthesis rate $k_{synt,MDM21} = 0.05\ min^{-1}$. $p53_i$ denotes unphosphorylated p53, $p53_a$ denotes p53-arrester phosphorylated at serine 15, $p53_k$ denotes p53-killer phosphorylated at serine 46.

III. RESULTS

A. DNA damage response exhibits distinct dynamics depending on parameter values and MYCN levels.

It is well established that the p53 DNA damage response system exhibits qualitatively distinct dynamics such as sustained and oscillatory responses in a cell-type, stimulus and dosage dependant manner [4]. For example, it was shown that UV radiation triggered a sustained p53 response, whereas gamma radiation resulted in oscillatory response dynamics. As one would expect form a system containing several positive and negative feedback loops, our model is well capable of simulating these different dynamic behaviours by changing the particular parameter values used in the simulations (Fig. 2). Because MYCN is intrinsically linked to the prognosis of Neuroblastoma patients, the parameter we were particularly interested in was the MYCN level. Interestingly, we observed that p53 response can switch from a sustained to an oscillatory response just by changing the level of MYCN (Fig. 2). Further, we observed that particularly high levels of MYCN markedly reduced the p53 response amplitude in our simulations. This is explored in more detail in the following.

B. p53 exhibits biphasic behaviour in response to MYCN.

An attractive hypothesis arising from the clinical data on MYCN described in the introduction is that the cancer cell fate and thus clinical outcome depends on the level of MYCN. Slightly increased levels of MYCN would promote cancer cell apoptosis, whereas hugely increased levels of MYCN would inhibit apoptosis. To test whether the p53-MYCN network (Fig. 1) is at least theoretically capable of exhibiting such a biphasic response, we simulated the model with increasing levels of MYCN (Fig. 3(a)). Our simulations show that p53 exhibits indeed a biphasic response to increasing MYCN levels; first increasing and then decreasing. Thus our computational analysis confirms that the p53-MYCN network is theoretically capable of explaining the dual, dosage-dependent MYCN effect.

C. Biphasic MYCN response does not depend on the dynamic regime.

Considering that the dynamic behaviour of the p53 system is highly context dependent and critically depends on the values of the kinetic parameters, we sought to investigate whether the above described biphasic MYCN response is robust. In particular, we asked whether the biphasic response can be observed in both the sustained and the oscillatory parameter regime. It is known that the oscillatory p53 dynamics depend on the mdm2-p53 negative feedback [29] and increasing this parameter in our model switches the response dynamics from sustained to oscillatory. Holding the MYCN-dependent MDM2 mRNA synthesis parameter ($k_{synt,MDM21}$) constant at a low value and increasing the level of MYCN switched the p53 responses from non-responding to sustained responses to non-responding (Fig. 3(a)). At intermediate $k_{synt,MDM21}$ values the system transitioned from non-responding to oscillatory responses and then to sustained responses with decreased amplitudes and finally switched off completely (Fig. 3(b)). For high $k_{synt,MDM21}$ the system switched directly from non-responding to oscillations, which then diminished in amplitude for further increasing MYCN values (Fig. 3(c)). Thus, the p53 system exhibited a robust biphasic MYCN response. In particular, the biphasic nature of this response was not dependent on whether the p53 system operated in the sustained or oscillatory parameter regime.

D. The HIPK2-HMGA1 interaction is crucial for the biphasic response.

Both the sustained and oscillatory regimes exhibited a biphasic response thus demonstrating that the biphasic behaviour is a robust result. But what is the underlying mechanism? Using simulations, we found that the MYCN mediated regulation of HMGA1, but not MDM2, caused the biphasic responses (Fig. 4). This can be intuitively explained as follows. On the one hand, moderately increased HMGA1 levels in response to slight MYCN increases lead to increased ATM expression, thus resulting in the activation of the ATM-HIPK2-p53 axis. On the other hand MYCN amplification causes excessive HMGA1 levels to an extent at which HMGA1 binds and sequesters HIPK2, thus inhibiting the pro-apoptotic phosphorylation of p53. Thus, MYCN-induced HMGA1 exhibits a dosage-dependent dual effect, first promoting the DNA damage response by inducing ATM, and then inhibiting the pro-apoptotic phosphorylation of p53 by sequestering HIPK2.

(a) $k_{synt,MDM21} = 0.01\ min^{-1}$

(b) $k_{synt,MDM21} = 0.05\ min^{-1}$
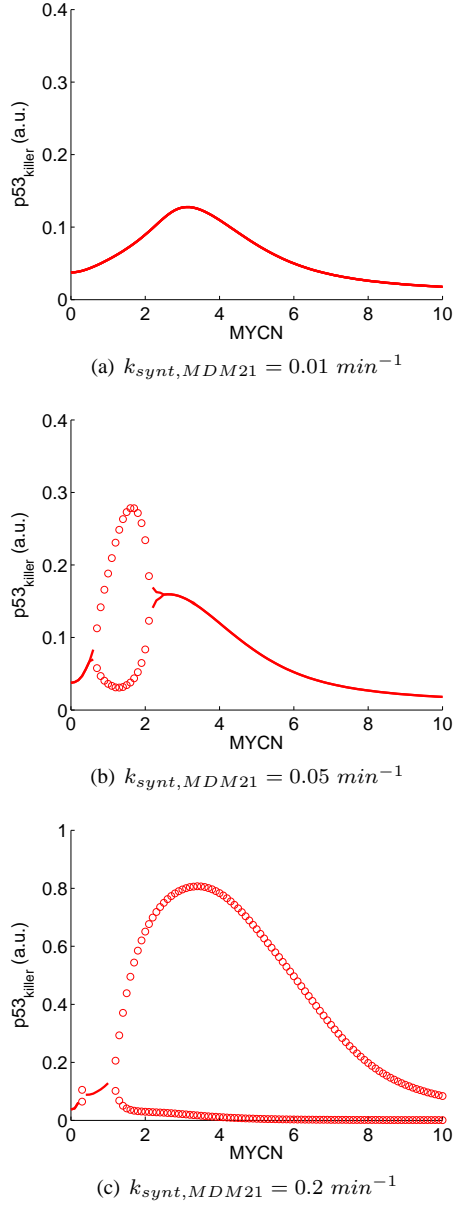

(c) $k_{synt,MDM21} = 0.2\ min^{-1}$

Fig. 3. Simulation showing the p53-killer response as a function of MYCN. The plot shows the asymptotic behaviour of the p53-killer response after DNA damage induction ($t > 2000$ min); solid lines indicate monostable steady-states values, circles the minimum and maximum of sustained oscillations.

E. Exploring different mechanisms of HMGA1-HIPK2 interaction.

The above results demonstrated a central role of HMGA1 for the cell fate decision in response to DNA damage. However, the HMGA1-HIPK2 interaction is not well characterised experimentally. For example, HMGA1 is phosphorylated by ATM [22] and this phosphorylation might promote or inhibit the interaction with HIPK2. We therefore explored these different possibilities in simulations using an ensemble of different models with different HMGA1-HIPK2 interactions patterns. We found that models in which HMGA1 does not bind HIPK2 or in which only the phosphorylated form of HMGA1 binds HIPK2 do not exhibit a biphasic MYCN response (Fig.

4(a),4(b)). In contrast, models in which only the unphosphorylated form of HMGA1 binds HIPK2 or in which HMGA1 binds irrespective of its phosphorylation status exhibited a biphasic response (Fig. 4(c),4(d)). Notably, the biphasic effect was most pronounced when only unphosphorylated HMGA1 bound HIPK2. These simulation results demonstrate that the nature of the MYCN-p53 response - biphasic or not - critically depends on the nature of the HMGA1-HIPK2 interaction. Further, these results provide a means of validating or invalidating the different possible biochemical mechanism of the HMGA1-HIPK2 interaction once experimental data on the MYCN-p53 response become available.

IV. CONCLUSIONS

Complex reaction networks are often difficult to understand intuitively making it necessary to describe and analyse them formally. The complexity of the present system lies in the multiple nested feedback loops within the p53 system, namely the ATM-p53-WIP1 and the p53-MDM2 feedbacks, and the dual role of HMGA1 which both positively regulates the ATM-p53 axis and negatively regulates the ATM-HIPK2-p53 axis. Here, we constructed a dynamic model of the p53 system that integrates a core network of the DNA damage response described in [5], [6] with extended knowledge about how MYCN affects the components within that system via its transcription factor activity. A key target of MYCN in our model is the gene HMGA1, which caused biphasic p53 responses for increasing MYCN levels in our simulations. This biphasic behaviour mimics the clinical pathology of MYCN neuroblastoma biology.

The prediction of the biphasic MYCN and HMGA1 behaviour can be validated experimentally by measuring the different components after DNA damage induction (drugs or radiation) in neuroblastoma cell lines, for example by Western blotting. Hereby, our model can be used to guide the experimental design. For example, to assess the effect of HMGA1 one experiment is to transfect a cell line expressing relatively low level of MYCN with increasing dosages of HMGA1 vector resulting in range of artificially induced HMGA1 expression levels. Observing a biphasic behaviour would be consistent with models (c) and (d) in Fig. 4, but not models (a) and (b). Vice-versa observing a monotone response would validate models (a) and (b). It is also possible to perform an experiment in a similar setup selecting a range of neuroblastoma cell lines naturally expressing different MYCN levels ranging from low to high, although different genetic backgrounds might limit the interpretation of this experiment.

The present model focused on MYCN feed forward effect which allowed us to use MYCN as an independent parameter. In a future work it will be of interest to investigate the feedback regulation of MYCN via MDM2 and p53 [30], [31]

In conclusion, our model allowed us to dissect complex dynamic behaviours related to MYCN biology and more specifically its dual role as pro-apoptotic and anti-apoptotic molecule. Simulation analyses allowed us to optimally design future experiments aimed at validating or invalidating the hypotheses generated by the model.

This model was deposited in BioModels Database [32] and assigned the identifier MODEL1410080001

REFERENCES

[1] M. Petroni, V. Veschi, A. Prodosmo, C. Rinaldo, I. Massimi, M. Carbonari, C. Dominici, H. McDowell, C. Rinaldi, I. Screpanti, L. Frati, A. Bartolazzi, A. Gulino, S. Soddu, and G. Giannini, "Mycn sensitizes human neuroblastoma to apoptosis by hipk2 activation through a dna damage response," *Molecular Cancer Research*, 2010.

[2] S. Peirce and H. Findley, "High level mycn expression in non-mycn amplified neuroblastoma is induced by the combination treatment nutlin-3 and doxorubicin and enhances chemosensitivity," *Oncology Reports*, 2009.

[3] H. Symonds, L. Krall, L. Remington, M. Saenz-Robles, S. Lowe, T. Jacks, and T. V. Dyke, "p53-dependent apoptosis suppresses tumor growth and progression in vivo," *Cell*, 1994.

[4] J. Purvis, K. Karhohs, C. Mock, E. Batchelor, A. Loewer, and G. Lahav, "p53 dynamics control cell fate," *Science*, 2012.

[5] T. Zhang, P. Brazhnik, and J. Tyson, "Computational analysis of dynamical responses to the intrinsic pathway of programmed cell death," *Biophysical Journal*, 2009.

[6] X. Zhang, F. Liu, and W. Wang, "Two-phase dynamics of p53 in the dna damage response," *Proceedings of National Academy of Sciences of the United States of America*, 2011.

[7] L. Smeenk, S. V. Heeringen, M. Koeppel, B. Gilbert, E. Janssen-Megens, H. Stunnenberg, and M. Lohrum, "Role of p53 serine 46 in p53 target gene regulation," *PLoS ONE*, 2011.

[8] J. Bartek and J. Lukas, "Dna repair: Damage alert," *Nature*, 2003.

[9] C. Bakkenist and M. Kastan, "Dna damage activates atm through intermolecular autophosphorylation and dimer dissociation," *Nature*, 2003.

[10] R. Khosravi, R. Maya, T. Gottlieb, M. Oren, Y. Shiloh, and D. Shkedy, "Rapid atm-dependent phosphorylation of mdm2 precedes p53 accumulation in response to dna damage," *Proceedings of National Academy of Sciences of the United States of America*, 1999.

[11] R. Maya, M. Balass, S.-T. Kim, D. Shkedy, J.-F. M. Leal, O. Shifman, M. Moas, T. Buschmann, Z. Ronai, Y. Shiloh, M. B. Kastan, E. Katzir, and M. Oren, "Atm-dependent phosphorylation of mdm2 on serine 395: role in p53 activation by dna damage," *Genes and Development*, 2001.

[12] M. Winter, D. Sombroek, I. Dauth, J. Moehlenbrink, K. Scheuermann, J. Crone, and T. Hofmann, "Control of hipk2 stability by ubiquitin ligase siah-1 and checkpoint kinases atm and atr," *Nature Cell Biology*, 2008.

[13] D. Choi, Y. Seo, E. Kim, K. Sung, J. Ahn, S. Park, S. Lee, and C. Choi, "Ubiquitination and degradation of homeodomain-interacting protein kinase 2 by wd40 repeat/socs box protein wsb-1," *Journal of Biological Chemistry*, 2008.

[14] C. Canman, D. Lim, K. Cimprich, Y. Taya, K. Tamai, K. Sakaguchi, E. Appella, M. Kastan, and J. Siliciano, "Activation of the atm kinase by ionizing radiation and phosphorylation of p53," *Science*, 1998.

[15] S. Banin, L. Moyal, S. Shieh, Y. Taya, C. Anderson, L. Chessa, N. Smorodinsky, C. Prives, Y. Reiss, Y. Shiloh, and Y. Ziv, "Enhanced phosphorylation of p53 by atm in response to dna damage," *Science*, 1998.

[16] A. Bode and Z. Dong, "Post-translational modification of p53 in tumorigenesis," *Nature Reviews Cancer*, 2004.

[17] G. D'Orazi, B. Cecchinelli, T. Bruno, I. Manni, Y. Higashimoto, S. Saito, M. Gostissa, S. Coen, A. Marchetti, G. D. Sal, G. Piaggio, M. Fanciulli, E. Appella, and S. Soddu, "Homeodomain-interacting protein kinase-2 phosphorylates p53 at ser 46 and mediates apoptosis," *Nature Cell Biology*, 2002.

[18] T. Hofmann, A. Mller, H. Sirma, H. Zentgraf, Y. Taya, W. Drge, H. Will, and M. Schmitz, "Regulation of p53 activity by its interaction with homeodomain-interacting protein kinase-2," *Nature Cell Biology*, 2002.

[19] S. Shreeram, O. Demidov, W. Hee, H. Yamaguchi, N. Onishi, C. Kek, O. Timofeev, C. Dudgeon, A. Fornace, C. Anderson, Y. Minami, E. Appella, and D. Bulavin, "Wip1 phosphatase modulates atm-dependent signaling pathways," *Molecular Cell*, 2006.

[20] X. Lu, B. Nannenga, and L. Donehower, "Ppm1d dephosphorylates chk1 and p53 and abrogates cell cycle checkpoints," *Genes and Development*, 2005.

[21] D. Palmieri, T. Valentino, D. D'Angelo, I. D. Martino, I. Postiglione, R. Pacelli, C. C. C. M. Fedele, and A. Fusco, "Hmga proteins promote atm expression and enhance cancer cell resistance to genotoxic agents," *Oncogene*, 2011.

[22] F. Pentimalli, D. Palmieri, R. Pacelli, C. Garbi, R. Cesari, E. Martin, G. Pierantoni, P. Chieffi, C. Croce, V. Costanzo, M. Fedele, and A. Fusco, "Hmga1 protein is a novel target of the atm kinase," *European Journal of Cancer*, 2008.

[23] G. Giannini, F. Cerignoli, M. Mellone, I. Massimi, C. Ambrosi, C. Rinaldi, C. Dominici, L. Frati, I. Screpanti, and A. Gulino, "High mobility group a1 is a molecular target for mycn in human neuroblastoma," *Cancer Research*, 2005.

[24] M. Petroni, V. Veschi, A. Gulino, and G. Giannini, "Molecular mechanisms of mycn-dependent apoptosis and the mdm2p53 pathway: an achilles heel to be exploited for the therapy of mycn-amplified neuroblastoma," *Frontiers in oncology*, 2012.

[25] G. Pierantoni, M. Fedele, F. Pentimalli, G. Benvenuto, R. Pero, G. Viglietto, M. Santoro, L. Chiariotti, and A. Fusco, "High mobility group i (y) proteins bind hipk2, a serine-threonine kinase protein which inhibits cell growth," *Nature Oncongene*, 2001.

[26] F. Esposito, M. Tornincasa, P. Chieffi, I. D. Martino, G. Pierantoni, and A. Fusco, "High-mobility group a1 proteins regulate p53-mediated transcription of bcl-2 gene," *Cancer Research*, 2010.

[27] A. Slack, Z. Chen, R. Tonelli, M. Pule, L. Hunt, A. Pession, and J. Shohet, "The p53 regulatory gene mdm2 is a direct transcriptional target of mycn in neuroblastoma," *Proceedings of National Academy of Sciences of the United States of America*, 2005.

[28] A. Polynikis, S. Hogan, and M. di Bernardo, "Comparing different ode modelling approaches for gene regulatory networks," *Journal of Theoretical Biology*, 2009.

[29] R. Bar-Or, R. Maya, L. Segel, U. Alon, A. Levine, and M. Oren, "Generation of oscillations by the p53-mdm2 feedback loop: A theoretical and experimental study," *Proceedings of the National Academy of Sciences*, 2000.

[30] L. Chen, N. Iraci, S. Gherardi, L. Gamble, K. Wood, G. Perini, J. Lunec, and D. Tweddle, "p53 is a direct transcriptional target of mycn in neuroblastoma," *Cancer Research*, 2010.

[31] J. He, L. Gu, H. Zhang, and M. Zhou, "Crosstalk between mycn and mdm2-p53 signal pathways regulates tumor cell growth and apoptosis in neuroblastoma," *Cell Cycle*, 2011.

[32] C. Li and al., "Biomodels database: An enhanced, curated and annotated resource for published quantitative kinetic models," *BMC Systems Biology*, 2010.
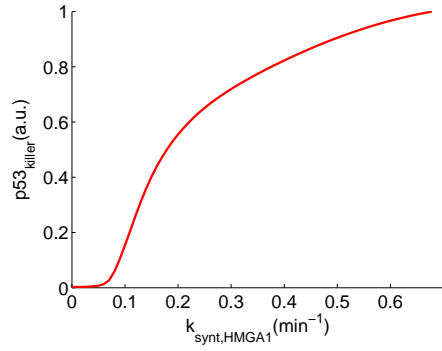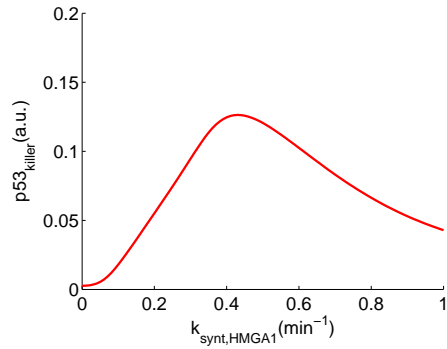
(a) $k_{1,HMGA1} = k_{1,HMGA1p} = 0$, none binds HIPK2
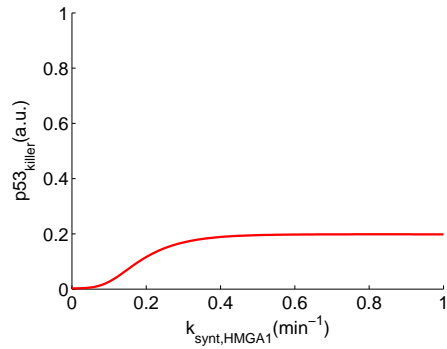
(b) $k_{1,HMGA1} = 0$, $k_{1,HMGA1p} = 4$, only HMGA1p binds HIPK2
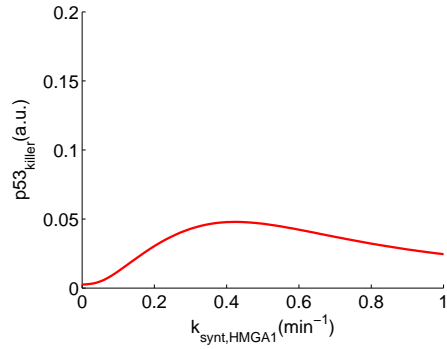
(c) $k_{1,HMGA1} = k_{1,HMGA1p} = 4$, both bind HIPK2

(d) $k_{1,HMGA1} = 4$, $k_{1,HMGA1p} = 0$, only HMGA1 binds HIPK2

Fig. 4. The biphasic response of p53 depends of the model structure and the nature of the HIPK2-HMGA1 interaction (a) HIPK2 does not bind HMGA1, (b) HIPK2 binds only the phosphorylated form of HMGA1, (c) HIPK2 binds both unphosphorylated and phosphorylated HMGA1, (d) HIPK2 binds only the non-phosphorylated form of HMGA1.

Reaction	Forward rate law	Reverse rate law	K_D	K_{-D}	k_1	k_{-1}
$[ATM] \xrightarrow{U_{DDR}} [ATM^*]$	$\frac{k_1 U_{DDR}}{U_{DDR}+k_{D1}} \times \frac{[ATM]}{[ATM+k_{D2}]}$	$\frac{k_{-1}[ATM^*][WIP1]}{k_{-D}+[ATM^*]}$	1, 5	2.3	10	2
$[p53] \xrightleftharpoons{[ATM^*]} [p53_{s15}]$	$\frac{k_1[p53][ATM^*]}{[p53]+k_D}$	$\frac{k_{-1}[p53_{s15}][WIP1]}{k_{-D}+[p53s15]}$	0.4	1.0	0.07	0.1
$[p53_{s15}] \xrightleftharpoons{[HIPK2]} [p53_{s46}]$	$\frac{k_1[p53_{s15}][HIPK2]}{[p53_{s15}]+k_D}$	$\frac{k_{-1}[p53_{s46}]}{k_{-D}+[p53_{s46}]}$	0.5	0.2	0.6	1.0
$[MDM2] \xrightleftharpoons{[ATM^*]} [MDM2_p]$	$\frac{k_1[MDM2][ATM^*]}{[MDM2]+k_D}$	$\frac{k_{-1}[MDM2_p]}{k_{-D}+[MDM2P]}$	0.1	0.1	0.1	0.1
$[HMGA1] \xrightleftharpoons{[ATM^*]} [HMGA1_p]$	$\frac{k_1[HMGA1][ATM^*]}{[HMGA1]+k_D}$	$\frac{k_{-1}[HMGA1_p]}{k_{-D}+[HMGA1P]}$	0.1	0.1	0.1	0.1
$[SIAH1] \xrightleftharpoons{[ATM^*]} [SIAH1_p]$	$\frac{k_1[SIAH1][ATM^*]}{[SIAH1]+k_D}$	$\frac{k_{-1}[SIAH1_p]}{k_{-D}+[SIAH1P]}$	0.1	0.1	0.1	0.1
$[HMGA1] + [HIPK2] \rightleftharpoons [HMGA1/HIPK2]$	$k_1[HMGA1][HIPK2]$	$k_{-1}[HMGA1/HIPK2]$	–	–	4*	2
$[HMGA1p] + [HIPK2] \rightleftharpoons [HMGA1p/HIPK2]$	$k_1[HMGA1p][HIPK2]$	$k_{-1}[HMGA1p/HIPK2]$	–	–	0**	2

* parameter varied in Fig. 4: $k_{1,HMGA1}$

** parameter varied in Fig. 4: $k_{1,HMGA1p}$

Reaction	Forward rate law	Reverse rate law	K	k_{synt}	k_{deg}
$\emptyset \rightleftharpoons [ATM_m]$	k_{synt}	$k_{deg}[ATM_m]$	–	0.1	0.1
$\emptyset \xrightarrow{[HMGA1]} [ATM_m]$	$\frac{k_{synt}[HMGA1]^2}{[HMGA1]^2+K^2}$	–	1	0.2	–
$\emptyset \xrightarrow{[HMGA1p]} [ATM_m]$	$\frac{k_{synt}[HMGA1p]^2}{[HMGA1p]^2+K^2}$	–	1	0.4	–
$\emptyset \rightleftharpoons [MDM2_m]$	k_{synt}	$k_{deg}[MDM2_m]$	–	0.002	0.003
$\emptyset \xrightarrow{[p53s15]+[p53s46]} [MDM2_m]$	$\frac{k_{synt}[p53_{s15}+p53_{s46}]^4}{[p53_{s15}+p53_{s46}]^4+K^4}$	–	1	0.024	–
$\emptyset \xrightarrow{[MYCN]} [MDM2_m]$	$\frac{k_{synt}[MYCN]^2}{[MYCN_p]^2+K^2}$	–	0.7	0.01*	–
$\emptyset \rightleftharpoons [WIP1_m]$	k_{synt}	$k_{deg}[WIP1_m]$	–	0.01	0.05
$\emptyset \xrightarrow{[p53s15]} [WIP1_m]$	$\frac{k_{synt}[p53_{s15}]^3}{[p53_{s15}]^3+K^3}$	–	0.5	0.1	–
$\emptyset \rightleftharpoons [HMGA1_m]$	k_{synt}	$k_{deg}[HMGA1_m]$	–	0.06	0.1
$\emptyset \xrightarrow{[MYCN]} [HMGA1_m]$	$\frac{k_{synt}[MYCN]^2}{[MYCN]^2+K^2}$	–	10	1.0	–

* the parameter varied in Fig. 3: $k_{synt,MDM21}$

Reaction	Forward rate law	Reverse rate law	k_{synt}	k_{deg}	K
$\emptyset \rightleftharpoons [p53]$	k_{synt}	$k_{deg}[p53]$	0.4	0.2	–
$[p53_{s15}] \rightarrow \emptyset$	–	$k_{deg}[p53_{s15}]$	–	0.1	–
$[p53_{s46}] \rightarrow \emptyset$	–	$k_{deg}[p53_{s46}]$	–	0.1	–
$\emptyset \rightleftharpoons [HIPK2]$	k_{synt}	$k_{deg}[HIPK2]$	0.4	0.1	–
$\emptyset \xrightleftharpoons{[HMGA1_m]} [HMGA1]$	$k_{synt}[HMGA1_m]$	$k_{deg}[HMGA1]$	0.2*	0.1	–
$[HMGA1_p] \rightarrow \emptyset$	–	$k_{deg}[HMGA1_p]$	–	0.1	–
$\emptyset \xrightleftharpoons{[WIP1_m]} [WIP1]$	$k_{synt}[WIP1_m]$	$k_{deg}[WIP1]$	0.2	0.05	–
$\emptyset \xrightleftharpoons{[ATM_m]} [ATM]$	$k_{synt}[ATM_m]$	$k_{deg}[ATM]$	0.1	0.1	–
$\emptyset \xrightleftharpoons{[MDM2_m]} [MDM2]$	$k_{synt}[MDM2_m]$	$k_{deg}[MDM2]$	0.004	0.003	–
$[MDM2_p] \rightarrow \emptyset$	–	$k_{deg}[MDM2_p]$	–	0.05	–
$[HMGA1/HIPK2] \rightarrow [HMGA1]$	$k_{deg}[HMGA1/HIPK2]$	–	–	0.1	–
$[HMGA1/HIPK2] \rightarrow [HIPK2]$	$k_{deg}[HMGA1/HIPK2]$	–	–	0.1	–
$[HMGA1p/HIPK2] \rightarrow [HMGA1p]$	$k_{deg}[HMGA1p/HIPK2]$	–	–	0.1	–
$[HMGA1p/HIPK2] \rightarrow [HIPK2]$	$k_{deg}[HMGA1p/HIPK2]$	–	–	0.1	–
$[p53] \xrightarrow{[MDM2]} \emptyset$	$\frac{k_{deg}[MDM2][p53]}{K+[p53]}$	–	–	0.1	1.0
$[HIPK2] \xrightarrow{[SIAH1]} \emptyset$	$\frac{k_{deg}[SIAH1][HIPK2]}{K+[HIPK2]}$	–	–	0.1	1.0

* the parameter varied in Fig. 4: $k_{synt,HMGA1}$

TABLE IV.   TABLE OF INITIAL VALUES

Variable	Description	Initial value
$[p53]$	Concentration of unphosphorylated p53 protein	0.8
$[p53_{s15}]$	Concentration of p53 phosphorylated at serine 15	0.1
$[p53_{s46}]$	Concentration of p53 phosphorylated at serine 46	0
$[SIAH1_p]$	Concentration of SIAH1 phosphorylated by ATM	0
$[HIPK2]$	Concentration of HIPK2 protein	0.2
$[WIP1_m]$	Concentration of WIP1 mRNA	0.2
$[WIP1]$	Concentration of WIP1 protein	0.2
$[HMGA1/HIPK2]$	Concentration of HMGA1/HIPK2 dimer	0.1
$[ATM^*]$	Concentration of ATM activated by DNA damage	0
$[HMGA1_p]$	Concentration of HMGA1 phosphorylated by ATM	0.1
$[ATM_m]$	Concentration of ATM mRNA	5
$[ATM]$	Concentration of ATM protein	5
$[HMGA1_m]$	Concentration of HMGA1 mRNA	1.0
$[HMGA1]$	Concentration of HMGA1 protein	1.0
$[MDM2_m]$	Concentration of MDM2 mRNA	0.26
$[MDM2]$	Concentration of MDM2 protein	0.26
$[MDM2_p]$	Concentration of MDM2 phosphorylated by ATM	0.4
$[HMGA1_p/HIPK2]$	Concentration of dimer of HMGA1 phosphorylated by ATM and HIPK2	0.1